

The Abduction of Sherlock Holmes: A Dataset for Visual Abductive Reasoning

Jack Hessel*♣ Jena D. Hwang*♣ Jae Sung Park♡ Rowan Zellers♡
Chandra Bhagavatula♣ Anna Rohrbach◇ Kate Saenko♠ Yejin Choi♣♡

♣Allen Institute for Artificial Intelligence

♡Paul G. Allen School of Computer Science & Engineering, University of Washington

◇University of California, Berkeley ♠ Boston University and MIT-IBM Watson AI

Abstract

Humans have remarkable capacity to reason abductively and hypothesize about what lies beyond the literal content of an image. By identifying concrete visual **clues** scattered throughout a scene, we almost can't help but draw probable **inferences** beyond the literal scene based on our everyday experience and knowledge about the world. For example, if we see a "20 mph" sign alongside a road, we might assume the street sits in a residential area (rather than on a highway), even if no houses are pictured. Can machines perform similar visual reasoning?

We present **SHERLOCK**, an annotated corpus of 103K images for testing machine capacity for **abductive** reasoning beyond literal image contents. We adopt a free-viewing paradigm: participants first observe and identify salient clues within images (e.g., objects, actions) and then provide a plausible inference about the scene, given the clue. In total, we collect 363K (clue, inference) pairs, which form a first-of-its-kind abductive visual reasoning dataset. Using our corpus, we test three complementary axes of abductive reasoning. We evaluate the capacity of models to: i) retrieve relevant inferences from a large candidate corpus; ii) localize evidence for inferences via bounding boxes, and iii) compare plausible inferences to match human judgments on a newly-collected diagnostic corpus of 19K Likert-scale judgments. While we find that fine-tuning CLIP-RN50×64 with a multitask objective outperforms strong baselines, significant headroom exists between model performance and human agreement. We provide analysis that points towards future work.

You know my method.
It is founded on the observation of trifles.

"The Boscombe Valley Mystery", by A. C. Doyle



Figure 1. We introduce **SHERLOCK**: a corpus of 363K common-sense inferences grounded in 103K images. Annotators highlight localized clues (color bubbles) and draw plausible abductive inferences about them (speech bubbles). Our models are able to predict localized inferences (top predictions are shown), but we quantify a large gap between machine performance and human agreement.

1. Introduction

The process of making the most plausible inference in the face of incomplete information is called *abductive reasoning*, [47] personified by the iconic visual inferences of the fictional detective Sherlock Holmes.¹ Upon viewing a

¹While Holmes rarely makes mistakes, he frequently misidentifies his mostly abductive process of reasoning as “deductive.” [8, 39]

scene, humans can quickly synthesize cues to arrive at abductive hypotheses that go beyond the literal scene captured in the frame. Concrete cues are diverse: we take into account the emotion and mood of the agents, speculate about the rationale for the presence/absence of objects, and zero-in on small, contextual details; all the while accounting for prior experiences and (potential mis)conceptions.² Figure 1 illustrates: snow may imply dangerous road conditions, an Ohio licence plate may suggest the location of the accident, and a blue sign may indicate this road is an interstate.

Though not all details are equally important, certain *salient* details shape our abductive inferences about the scene as a whole [56]. This type of visual information is often left unstated. Prior work on resources including Visual Commonsense Reasoning [75] and VisualCOMET [44], has mostly focused on making direct inferences about what humans are doing.³ On the other hand, as humans, we can go beyond this—making global scene inferences *abductively* from salient objects in the scene, that in turn reframe our understanding of what people are doing. For instance, observing the semitruck lying in the freeway in Figure 1 suggests that there was a major accident that occurred just recently, which in turn frames our understanding of what the workers in the yellow vests are doing.

We introduce **SHERLOCK**, a new dataset of 363K commonsense inferences grounded in 103K images. **SHERLOCK** makes explicit typically-unstated cognitive processes: each image is annotated with at least 3 inferences which pair depicted details (called clues) with commonsense conclusions that aim to go *beyond* what is literally pictured (called inferences). Going beyond existing visual commonsense corpora, **SHERLOCK** is more diverse, due to its free-viewing data collection paradigm: we purposefully do not pre-specify the types of clues/inferences allowed, and leave it to humans to identify the most salient elements (and their implications). In contrast, image captions, another form of free-viewing, are not enough: returning to Figure 1, a typical image caption may mention the accident (and perhaps the icy conditions), but smaller details (like the blue freeway sign or the Ohio plates) may not be mentioned explicitly [5]. Dense captioning corpora [22] aim to highlight *all* details, but do not account for which are salient (and why).

Using our corpus, we propose three complementary tasks that evaluate different aspects of machine capacity for visual abductive reasoning:

1. *Retrieval of Abductive Inferences*: given an image+region, the algorithm scores a large set of candidate

²As even Sherlock himself could attest, the *correctness* of abductive reasoning is certainly not guaranteed. Our goal is to study perception and reasoning *without* endorsing specific inferences. See §3.2 for a discussion of intended use-cases for our corpus.

³For instance, 94% of visual references in [75] are about depicted actors, and [44] even requires KB entries to explicitly regard people.

inferences and is rewarded for assigning a high score to the gold annotation.

2. *Localization of Evidence*: the algorithm selects a bounding box within the image that provides the best evidence for a given inference.
3. *Comparison of Plausibility*: the algorithm scores a small set of plausible inferences for a given image+region, and is rewarded for aligning its scores with human judgments over those sets.

In our setup, a single model undertakes all of these tasks: we ask algorithms to score the plausibility of an inference given an image and a bounding box contained within it.

Predicted inferences of one of our best performing models are given in Figure 1. The model itself a fine-tuned CLIP [51], augmented to allow bounding boxes as input: this enables the user to specify particular regions for the model to make abductive inferences about. Our best model, a multitask version of CLIP RN50×64, outperforms strong baselines like UNITER [9] and LXMERT [61] primarily because it is able to pay specific attention to the correct input bounding box. We additionally show that 1) for all tasks, reasoning about the full context of the image (rather than just the region corresponding to the clue) results in the best performance; and 2) a text-only model cannot solve the comparison task; and 3) a multi-task model fit on both clues/inferences at training time performs best even when only inferences are available at test time.

We foresee **SHERLOCK** as a difficult diagnostic benchmark for vision-and-language models. On our comparison task, in terms of pairwise accuracy, our best model lags significantly below human agreement (headroom also exists for retrieval and localization). We release code, data, and models at visualabduction.com

2. Related Work

Abductive reasoning. Abduction is a form of everyday reasoning first framed by C. S. Peirce; [46, 47]; in essence, an abductive inference is an explanatory hypothesis—a “best” guess — based on limited evidence. Humans use abduction to reconcile seemingly disconnected observations to arrive at meaningful conclusions [56] but readily retract in presence of new evidence [1]. In linguistics, the process of abduction for communicated meaning (in an impoverished conversational context) is systematized through conversational maxims [15]. In images, [5] show that different object types have different likelihoods of being mentioned in image captions (e.g., “fireworks” is always mentioned if depicted, but “fabric” is not), but that object type alone does not dictate salience for abductive inferences, e.g., a TV in a living room may not be as conceptually salient as a TV in a bar, which may signal a particular type of bar. Abductive reasoning has recently received attention in language processing tasks [6, 11, 45, 50], proof writing [60], and dis-

Dataset	# Images	Format	bboxes?	free-viewing?	human-centric?
VCR [75]	110K	QA	✓		✓
VisualCOMET [44]	59K	If/Then KB	✓		✓
Visual7W [80]	47K	QA	✓	partial	
Visual Madlibs [72]	11K	FiTB	✓	partial	✓
Abstract Scenes [65]	4.3K	KB			
Why In Images [49]	792	KB			✓
BD2BB [48]	3.2K	If/Then		✓	✓
FVQA [66]	2.2K	QA+KB			
OK-VQA [36]	14K	QA		✓	
KB-VQA [67]	700	QA	✓		
SHERLOCK	103K	clue/inference	✓	✓	

Table 1. Comparison between **SHERLOCK** and prior annotated corpora addressing visual abductive reasoning from static images. **SHERLOCK** showcases a unique clue/inference data collection paradigm, leading to a rich variety of non-human centric (i.e., not solely grounded in human references) visual abductive inferences.

course processing [17, 42], among other contexts.

Beyond visual recognition. Visual understanding and reasoning that go beyond descriptive content have gained increasing attention, including work on visual and analogical reasoning [3, 21, 43, 77], scene graphs and semantics [23], commonsense interactions [49, 65], temporal/causal reasoning [71], and perceived importance [5]. Some prior work has explored commonsense reasoning tasks posed over videos, which usually have more input available than a single frame [12, 13, 19, 20, 30, 31, 33, 63, 74, 78] (inter alia).

Visual abductive reasoning. **SHERLOCK** builds upon prior grounded visual abductive reasoning efforts (Table 1). Corpora like Visual Commonsense Reasoning (VCR) [75], VisualCOMET [44], and Visual7W [80] are most similar to **SHERLOCK** in providing benchmarks for rationale-based inferences (i.e., the why and how). But, **SHERLOCK** differs in format and content (Table 2). Instead of annotated QA pairs like in [75, 80] where one option is definitively correct, free-text clue/inference pairs allow for broader types of image descriptions, lending itself to softer and richer notions of reasoning (see §4)—inferences are not definitively correct vs. incorrect, rather, they span a range of plausibility. Deviating from the constrained, human-centric annotation of [44], **SHERLOCK** clue/inference pairs support a broader range of topics via our free-viewing (open-ended) annotation paradigm (see §3.1). **SHERLOCK**’s inferences can be grounded on any number of visual objects in an image, from figures central to the image (e.g., persons, animals, objects) to the miscellaneous background cues that indicate the setting of the image (e.g., time, location, circumstances).

3. SHERLOCK Corpus

The **SHERLOCK** corpus contains a total of 363K abductive commonsense inferences grounded in 81K Visual Genome



Visual Commonsense Reasoning (VCR) [75]

Question: What is Person1 doing?

(1) He is dancing. (2) He is giving a speech. (3) Person1 is getting his medicine. (4) **He is ordering a drink from Person5.**

Visual COMET [44]

Event: Person5 mans the register and takes order

Before Person5 needed to write down orders

Because Person5 wanted to have everyone pay for their orders

SHERLOCK

Clue A: a beer sign on the wall → Alcohol is served here

Clue B: USD hanging on a pitcher → This is the USA

Table 2. Side-by-side comparison of VCR, VisualCOMET, and **SHERLOCK** on a representative instance. In addition to format differences (Table 1), VCR and VisualCOMET’s visual references focus primarily on humans (94% and 100% of references, respectively) vs. only 36% for **SHERLOCK**. As a result, **SHERLOCK** captures a wider range of situational contexts.

[28] images (photographs from Flickr) and 22K Visual Commonsense Reasoning (VCR) [75] images (still-frames from movies). Images have an average of 3.5 OBSERVATION PAIRS, which each consist of

- **clue:** an observable entity or object in the image, along with bounding box(es) specifying it (e.g., “people wearing nametags”).
- **inference:** an abductive inference associated with the clue; not immediately obvious from the image content (e.g., “the people don’t know each other”).

Both clues and inferences are represented via free text in English; both have an average length of seven tokens; per clue, there are a mean/median of 1.17/1.0 bounding boxes per clue. We divide the 103K annotated images into a training/validation/test set of 90K/6.6K/6.6K. Further details are available in §A.2.

3.1. Dataset Collection

Annotation process. We crowdsource our dataset via Amazon Mechanical Turk. For each data collection HIT, a worker is given an image and prompted for 3 to 5 OBSER-

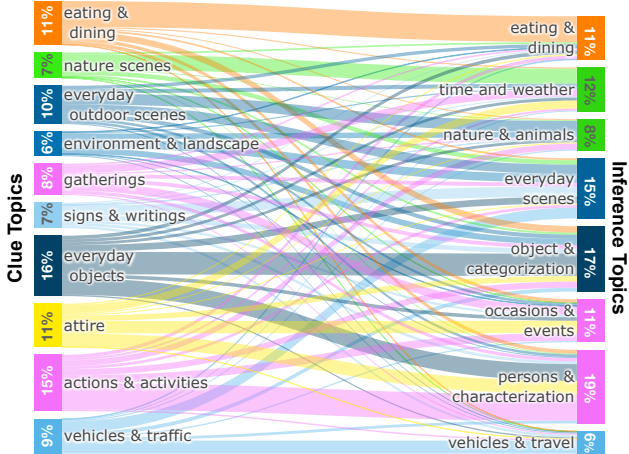


Figure 2. Overview of the topics represented in the clues and inferences in **SHERLOCK**. This analysis shows that **SHERLOCK** covers a variety of topics commonly accessible in the natural world. Color of the connections reflect the clue topic.

VATION PAIRS. For each OBSERVATION PAIR, the worker is asked to write a clue, highlight the regions in the image corresponding to the clue, and write an inference triggered by the clue. To encourage abductive reasoning rather than purely deductive reasoning, the workers are actively encouraged to think beyond the literally depicted scene, while staying within the realm of real-world expectations. To ensure annotator quality, the HITs were worked on by 266 manually qualified workers. Annotators were paid \$15/hr; further details on the annotation process are provided in §A.

3.2. Dataset Exploration

SHERLOCK contains abductive inferences that cover a wide variety of real world experiences: from observations about unseen (but probable) details of the image (e.g., “smoke at an outdoor gathering” → “something is being grilled”), to cases that elaborate on the expected social context (e.g., “people wearing nametags” → “the people don’t know each other”). Some inferences are highly likely to be true (e.g., “wet pavement” → “it has rained recently”); others are less definitively verifiable, but nonetheless plausible (e.g., “large trash containers” → “there is a business nearby”). Through a rich array of natural observations, **SHERLOCK** provides a tangible view into the abductive inferences people use on an everyday basis. More examples are given in the Appendix (Figure 11).

Assessing topic diversity. To gauge the diversity of objects and situations represented in **SHERLOCK**, we run a topic model (LDA [7]) over the clues and inferences. Figure 2 shows the topics of the clues and inferences; they span a range of common everyday objects, entities, and situations. We also observe that inference topics associated with the

clues include categorical associations (e.g., “baked potatoes on a ceramic plate” → “this will be served as a side dish”) and boundary-crossing associations (e.g., “a nametag” (attire) → “she works here” (characterization)). Many topics are not human centric; compared to VCR in which 94% of grounded references are to people,⁴ a manual analysis of 150 clues reveals that only 36% of **SHERLOCK** OBSERVATION PAIRS are grounded on people.

Intended use cases. We manually examine of 250 randomly sampled OBSERVATION PAIRS to better understand how annotators referenced protected characteristics (e.g., gender, color, nationality) A majority of inferences (243/250) are not directly about protected characteristics, though, a perceived gender is often made explicit via pronoun usage, e.g., “she is running.” As an additional check, we pass 30K samples of our corpus through the Perspective API.⁵ A manual examination of 150 cases marked as “most toxic” reveals mostly false positives (89%), though 11% of this sample do contain lewd content (mostly prompted by the visual content in the R-rated VCR movies) or stigmas related to, e.g., gender and weight. See §A.4 for a more complete discussion.

While our analysis suggests that the relative magnitude of potentially offensive content is low in **SHERLOCK**, we still advocate against deployed use-cases that run the risk of perpetuating potential biases: our aim is to study abductive reasoning without endorsing the correctness or appropriateness of particular inferences. We foresee **SHERLOCK** as 1) a diagnostic corpus for measuring machine capacity for visual abductive reasoning; 2) a large-scale resource to study the types of inferences people may make about images; and 3) a potentially helpful resource for building tools that require understanding *abductions* specifically, e.g., for detecting purposefully manipulative content posted online, it could be useful to specifically study what people *might assume* about an image (rather than what is objectively correct; more details in Datasheet (§D) [14]).

4. From Images to Abductive Inferences

We operationalize our corpus with three tasks, which we call retrieval, localization, and comparison. Notationally, we say that an instance within the **SHERLOCK** corpus consists of an image i , a region specified by N bounding boxes $\mathbf{r} = \{ \langle x_{1i}, x_{2i}, y_{1i}, y_{2i} \rangle \}_{i=1}^N$,⁶ a clue c corresponding to a literal description of \mathbf{r} ’s contents, and an **inF**erence f that

⁴In VisualCOMET, all KB entries are centered around people.

⁵<https://www.perspectiveapi.com/>; November 2021 version. The API (which itself is imperfect and has biases [18,38,55]) assigns toxicity value 0-1 for a given input text. Toxicity is defined as “a rude, disrespectful, or unreasonable comment that is likely to make one leave a discussion.”

⁶As discussed in §3.1, N has a mean/median of 1.17/1.0 across the corpus.

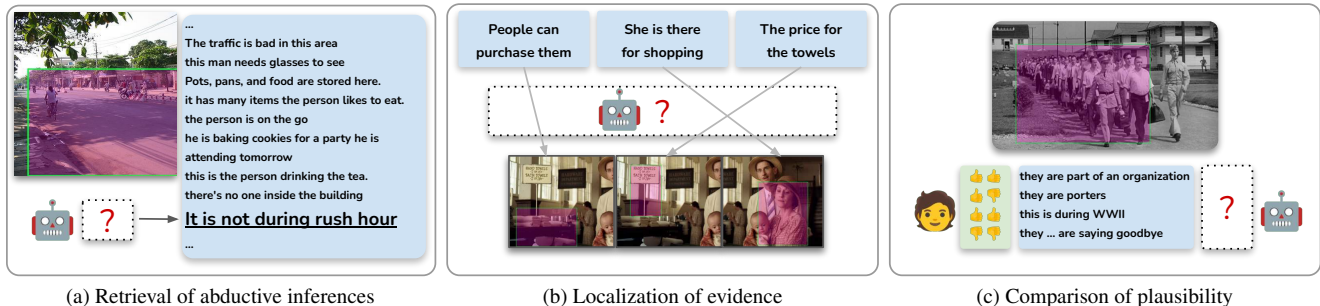


Figure 3. Illustration of the tasks we consider posed over the **SHERLOCK** corpus. In *retrieval*, models are tasked with finding the ground-truth inference across a wide range of inferences, some much more plausible/relevant than others. In *localization*, models must align regions within the same image to several inferences written about that image. For *comparison*, we collect **19K Likert ratings** from human raters across **plausible candidates**, and models are evaluated in their capacity to reconstruct human judgments across the candidates. While all tasks have some intrinsic subjectivity, headroom exists, e.g., between human agreement and model performance on the *comparison* task.

an annotator associated with i , r , and c . We study the following tasks:

1. *Retrieval of Abductive Inferences*: For a given image/region pair (i, r) , how well can models select the ground-truth inference f from a large set of candidates ($\sim 1K$) covering a broad swath of the corpus?
2. *Localization of Evidence*: Given an image i and an inference f written about an (unknown) region within the image, how well can models locate the proper region?
3. *Comparison of Plausibility*: Given an image/region pair (i, r) and a small set (~ 10) of relevant inferences, can models predict how humans will rank their plausibility?

Figure 3 illustrates how each task tests a complementary aspect of visual abductive reasoning: retrieval tests across a broad range of inferences, localization tests within-images, and comparison tests for correlation with human judgement. Nonetheless, the *same* model can undertake all three tasks if it implements the following interface:

SHERLOCK Abductive Visual Reasoning Interface

- **Input:** An image i , a region r within the image, and a candidate inference f .
- **Target:** A score s , where s is proportional to the plausibility that f could be inferred from (i, r) .

That is, we assume a model $m : (i, r, f) \rightarrow \mathbb{R}$ that scores inference f 's plausibility for (i, r) . Notably, the interface takes as input inferences, but not clues: our intent is to focus evaluation on abductive reasoning, rather than the distinct setting of literal referring expressions.⁷ Clues can be used for training m ; as we will see in §5, our best performing model, in fact, does use clues at training time.

⁷In §B.1, for completeness, we give results on the retrieval and localization setups, but testing on clues instead.

4.1. Retrieval of Abductive Inferences

For retrieval evaluation, at test time, we are given an (i, r) pair, and a large ($\sim 1K$)⁸ set of candidate inferences $f \in \mathcal{F}$, only one of which was written by an annotator for (i, r) ; the others are randomly sampled from the corpus. In the $im \rightarrow txt$ direction, we compute the mean rank of the true item (lower=better) and $P@1$ (higher=better). Also, because retrieval over commonsense inferences is not one-to-one, some mistakes are more justifiable than others. Consider the example from Figure 1 with the clue “large semi truck and trailer on its side laying on a freeway.” While the author inferred from the clue that a “major accident ... occurred minutes ago,” we would like to assign more credit if a model were to select (the lexically dissimilar) “the wreck will cause traffic”, than if it selected “This watch displays minutes”. For perspective beyond hard retrieval metrics, we also consider the BERTScore [79]⁹ of the retrieved inferences, computed using the ground-truth inference as a (single) reference. Finally, because the retrieval setup is symmetric, we also report one $txt \rightarrow im$ direction metric: mean rank (lower=better).

4.2. Localization of Evidence

We next consider localization, which assesses a model’s capacity select a regions within an image that most directly supports a given inference. Following prior work on literal referring expression localization [25, 27, 73] (inter alia), we experiment in two settings: 1) we are given all the ground-truth bounding boxes for an image, and 2) we are given only automatic bounding box proposals from an object detection model.

GT bounding boxes. We assume an image i , the set of

⁸Our validation/test sets contain about 23K inferences. For efficiency we randomly split into 23 equal sized chunks of about 1K inferences, and report retrieval averaged over the resulting splits.

⁹We use RoBERTa-Large [34] with rescaling and no IDF.

3+ inferences F written for that image, and the (unaligned) set of regions R corresponding to F . The model must produce a one-to-one assignment of F to R in the context of i . In practice, we score all possible $F \times R$ pairs via the abductive visual reasoning interface, and then compute the maximum linear assignment [29] using `lapjv`’s implementation of [24]. The evaluation metric is the accuracy of this assignment, averaged over all images. To quantify an upper bound, a human rater performed the assignment for 101 images, achieving an average accuracy of 92.3%.

Auto bounding boxes. We compute 100 bounding box proposals per image by applying Faster-RCNN [54] with a ResNeXt101 [69] backbone trained on Visual Genome to all the images in our corpus. Given an image i and an inference f that was written about the image, we score all 100 bounding box proposals independently, and take the highest scoring one as the prediction. We count a prediction as correct if it has IoU > 0.5 with a true bounding box that corresponds to that inference,¹⁰ and incorrect otherwise.¹¹

4.3. Comparison of Plausibility

We seek to assess model capacity to make fine-grained assessments given a set of plausible inferences. For example, in Figure 3c (depicting a group of men marching and carrying bags), human raters are *likely* to say that these are military men and that the photo was taken during WWII, and *unlikely* to see them as porters despite them carrying bags.¹² Our evaluation assumes that a performant model’s predictions should correlate with the (average) relative judgments that humans make, and we seek to construct a corpus that supports evaluation of such reasoning.

Constructing sets of plausible inferences. It is combinatorially prohibitive to gather human judgements for all possible image/inference pairs in our corpus. Furthermore, randomly sampling from all pairs as in *retrieval* would produce many obviously irrelevant/wrong cases. To form sets of plausible inferences, we use a performant model checkpoint fine-tuned for the Sherlock tasks.¹³ Then, we use this model to compute the similarity score between all (i, r, f) triples in the validation/test sets. Next, we perform several filtering steps: 1) we only consider pairs where the negative inference received a higher score than the ground-truth according to the model; 2) we perform soft text deduplication to downsample inferences that are semantically similar;

¹⁰Since the annotators were able to specify multiple bounding boxes per OBSERVATION PAIR, we count a match to any of the labeled bounding boxes.

¹¹A small number of images do not have a ResNeXt bounding box with IoU > 0.5 with any ground truth bounding box: in §5.1, we show that most instances (96.2%) are solvable with this setup.

¹²Porters are employed to carry baggage at airports, hotels, etc.

¹³Specifically, a CLIP RN50x16 checkpoint that achieves strong validation retrieval performance (comparable to the checkpoint we report the test results of in §5.1); model details in §5.

and 3) we perform hard text deduplication, only allowing inferences to appear verbatim 3x times. Then, through an iterative process, we uniquely sample a diverse set of 10 inferences per (i, r) that meet these filtering criteria. This results in a set of 10 plausible inference candidates for each of 485/472 validation/test images. More details are in §C. In a retrieval sense, these plausible inferences can be viewed as “hard negatives:” i.e., none are the ground-truth inference, but a strong model nonetheless rates them as plausible.

Human rating of plausible inferences. We collect two annotations of each candidate inference on a three-point Likert scale ranging from 1 (bad: “irrelevant”/“verifiably incorrect”) to 3 (good: “statement is probably true; the highlighted region supports it.”). Full rating criteria and details of filtering are in §C. We collect 19K annotations in total. Because abductive reasoning involves subjectivity and uncertainty, we expect some amount of intrinsic disagreement between raters (in §5.1, we show that models achieve significantly less correlation compared to human agreement). We measure model correlation with human judgments on this set via pairwise accuracy. For each image, for all pairs of candidates that are rated differently on the Likert scale, the model gets an accuracy point if it orders them consistently with the human rater’s ordering. Ties are broken randomly and consistently across all models. For readability, we subtract the accuracy of a random model (50%) and multiply by two to form the final accuracy metric.

5. Experiments

Training objective. We seek models that support the interface described in §4, i.e., we train models $m : (i, r, f) \rightarrow \mathbb{R}$ that score inference f ’s plausibility for (i, r) . While we experiment with several different V+L backbones as detailed below, for each, we train by optimizing model parameters to score truly corresponding (i, r, f) triples more highly than negatively sampled (i, r, f_{fake}) triples.

LXMERT. [61] is a vision+language transformer [64] model pre-trained on Visual Genome [28] and MSCOCO [32]. The model is composed of three transformer encoders [64]: an object-relationship encoder (which takes in ROI features+locations, with a max of 36, following [2]), a language encoder that processes word tokens, and a cross modality encoder that learns the joint representation. To provide region information r to the visual encoder, we calculate the ROI feature of r and always place it in the first object token (this is a common practice for, e.g., the VCR dataset [75]). We follow [9] to train the model in “image-text retrieval” mode by maximizing the margin $m = .2$ between the cosine similarity scores of positive triple (i, r, f) and two negative triples (i, r, f_{fake}) and (i_{fake}, r_{fake}, f) through triplet loss.

UNITER. [9] similarly takes in object-level features and

	Retrieval			Localization		Comparison
	im \rightarrow txt (\downarrow)	txt \rightarrow im (\downarrow)	$P@1_{im \rightarrow txt}$ (\uparrow)	BERTScore (\uparrow)	GT-Box/Auto-Box (\uparrow)	Val/Test Human Acc (\uparrow)
Random	495.4	495.4	0.1	14.5	30.0/7.9	1.1/-0.6
Bbox Position/Size	257.5	262.7	1.3	15.6	57.3/18.8	5.5/1.4
LXMERT	51.1	48.8	14.9	22.7	69.5/30.3	18.6/21.1
UNITER Base	40.4	40.0	19.8	23.3	73.0/33.3	20.0/22.9
CLIP ViT-B/16	19.9	21.6	30.5	24.0	85.3/38.6	20.1/21.2
CLIP RN50x16	19.3	20.8	31.0	23.7	85.7/38.7	21.6/23.7
CLIP RN50x64	19.3	19.7	31.8	24.1	86.6/39.5	25.1/26.0
\downarrow + multitask clue learning	16.4	17.9	33.4	24.3	87.2/40.6	26.6/27.1
Text-only T5-Large	-	-	-	-	-	22.8/19.3
Human + (Upper Bound)	-	-	-	-	92.3/(96.2)	42.3/42.3

Table 3. Test results for all models across all three tasks. CLIP RN50x64 outperforms all models in all setups, but significant headroom exists, e.g., on Comparison between the model and human agreement.

word tokens as input to learn the cross-modal embedding. Unlike LXMERT [61], it consists of a single, unified transformer that takes in image and text embeddings. We experiment with the Base version pre-trained on MSCOCO [32], Visual Genome [28], Conceptual Captions [57], and SBU Captions [41]. We apply the same strategy of region-of-reference-first passing, and train with the same triplet loss following [9].

CLIP. We finetune the ViT-B/16, RN50x16, and RN50x50 versions of CLIP [51]. Text is represented via a 12-layer text transformer. For ViT-B/16, images are represented by a 12-layer vision transformer [10], whereas for RN50x16/RN50x64, images are represented by ResNet50 [16] scaled up to have 16x/64x the compute according to the EfficientNet scaling protocol [62].

We modify CLIP so that it can incorporate the bounding box as input: inspired by a similar process from [70, 76], to pass a region to CLIP, we simply draw a bounding box on an image in pixel space—we use a green-bordered / opaque purple box as depicted in Figure 4b (this proved more effective than modifying CLIP’s architecture). To enable CLIP to process the widescreen images of VCR, we apply it twice to the input using overlapping square regions, i.e., graphically, like this: $[\begin{smallmatrix} 1 & [2] \\ [2] & 1 \end{smallmatrix}]_2$, and average the resulting embeddings. We fine-tune using InfoNCE [40, 59]. We sample a batch of truly corresponding (i, r, f) triples, render the regions r in their corresponding images, and then construct all possible negative (i, r, f_{fake}) triples in the batch by aligning each inference to each (i, r) . The batch size controls the number of negative cases the model sees during training. We use the biggest minibatch size possible using 8 GPUs with 48GB of memory each: 64, 200, and 512 for RN50x64, RN50x16, and ViT-B/16, respectively.

Multitask learning. All models thusfar only utilize inferences at training time. We experiment with a multitask learning setup using CLIP that additionally trains with clues. In addition to training using our abductive reason-

ing objective, i.e., InfoNCE on inferences, we mix in an additional referring expression objective, i.e., InfoNCE on clues. Evaluation remains the same: at test time, we do not assume access to clues. At training time, for each observation, half the time we sample an inference (to form (i, r, f)), and half the time we sample a clue (to form (i, r, c)). The clue/inference mixed batch of examples is then handed to CLIP, and a gradient update is made with InfoNCE as usual. To enable to model to differentiate between clues/inferences, we prefix the texts with `clue:/inference:`, respectively.

Baselines. In addition to a random baseline, we consider a content-free version of our CLIP ViT-B/16 model that is given only the position/size of each bounding box. While more details are given in §5.2, in place of the image, we pass a mean pixel value across the entire image, and draw the bounding box on the image using an opaque pink box.

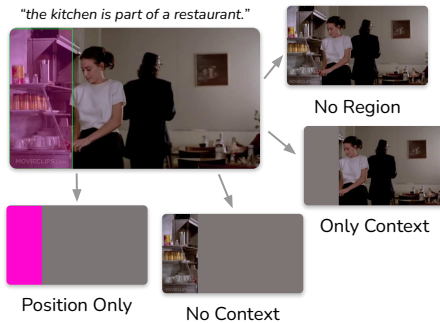
5.1. Results

Table 3 contains the results for all the retrieval, localization, and comparison evaluations. In all cases, our CLIP-based models perform best, with RN50x64 outperforming its smaller counterparts. Incorporating the multitask objective pushes performance further. While CLIP performs the best, UNITER is more competitive on comparison and less competitive on retrieval and localization. We speculate this has to do with the nature of each task: Retrieval requires models to reason about many incorrect examples, whereas, the inferences in the comparison task are usually relevant to the objects in the scene. While UNITER is more competitive in making fine-grained distinctions between two reasonable cases, when queried with a lower quality instance, it’s less precise in assigning a low score.

Batch size. Because UNITER/LXMERT are bidirectional, they are quadratically more memory intensive vs. CLIP: as a result, for those models, we were only able to train with 18 negative examples per positive (c.f. CLIP

	$P@1$ (\uparrow)	Val/Test Human (\uparrow)
CLIP ViT-B/16	30.5	20.1/21.2
input		
↳ Position only	1.3	5.5/1.4
↳ No Region	18.1	16.8/19.0
↳ No Context	24.8	18.1/17.8
↳ Only context	18.9	17.4/16.3
↳ Trained w/ only Clues	23.0	16.2/19.7
model		
↳ Crop no Widescreen	27.8	23.1/21.8
↳ Resize no Widescreen	27.7	19.4/20.6
↳ Zero shot w/ prompt	12.0	10.0/9.5

(a)



(b)

Figure 4. We perform ablations by varying the input data, top (a), and the modeling components, bottom (a). Figure (b) depicts our image input ablations, which are conducted by drawing in pixel-space directly, following [76]. Having no context may make it difficult to situate the scene more broadly; here: neatly stacked cups could be in a bar, a hotel, a store, etc. Access only the context of the dining room is also insufficient. For modeling, bottom (a), cropping/resizing decreases performance on retrieval ($P@1$), but not comparison (Val/Test Human).

ViT-B/16, which uses 511 negatives). To check that batch size/number of negatives wasn’t the only reason CLIP outperformed UNITER, we conducted an experiment varying ViT-B/16’s batch size from 4 to 512; the results are given in Figure 5. Batch size doesn’t explain all performance differences: with a batch size of only 4, our weakest CLIP-based model still localizes better than UNITER, and, at batch size 8, it surpasses UNITER’s retrieval performance.

5.2. Ablations

We perform two types of ablations on CLIP ViT-B/16: data ablations and model ablations. The results are in Figure 4a.

Input ablations. Each part of our visual input is important; aside from the position only model, the biggest drop-off in performance results from not passing the region as input to CLIP, e.g., $P@1$ for $im \rightarrow txt$ retrieval nearly halves, dropping from 31 to 18; this suggests that CLIP relies on the local region information to reason about the image. Removing the region’s content (“Only Context”) unsurprisingly hurts performance, but so does removing the surrounding context (“No Context”); indeed, the model performs the best when it can reason about the clue and its full visual context jointly. On the text side, we trained a model with only clues; retrieval and comparison performance both drop, which suggests that clues and inferences carry different information (additional supporting results in §B.1).

Model ablations. We considered two alternate image processing configurations. Instead of doing two CLIP passes per image to facilitate widescreen processing (as described in §5), we consider i) center cropping and ii) pad-and-resizing. Both take less computation, but provide less information to the model. Cropping removes the sides of images,

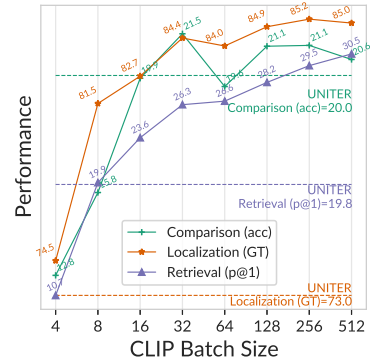


Figure 5. The effect of CLIP batch size (=number of negatives+1) on performance of ViT-B-16. UNITER is trained with 18 negatives per example. Performance on all tasks increases with increasing batch size, but appears to saturate, particularly for the comparison task.

whereas pad-and-resize lowers the resolution significantly. The bottom half of the table in Figure 4a reports the results: both configurations lower performance on retrieval tasks, but there’s less impact for comparison.

Better retrieval → better comparison. In Figure 6, we correlate the retrieval performance of our (single-task) CLIP model checkpoints with the human-agreement of those checkpoints attained for our comparison task. Even when controlling for model architecture, we see a high correlation between retrieval performance (as measured by $P@1$) and how well the model predictions are correlated with human judgement on the comparison task. For the smaller RN50×16 and ViT-B/16 models, this effect cannot simply be explained by training time. For RN50×16, the pearson correlation between training steps and reasoning performance is 81, whereas, the correlation between $P@1$ and reasoning performance is 91. While a significant gap exists between machine performance and human agreement for all models, it’s plausible that a model with higher precision at retrieval could help further bridge the gap.

Text-only models are insufficient. One potential concern with our setup is that clues may map deterministically and one-to-one onto inferences, e.g., if all soccer balls in our corpus were mapped onto “the owner plays soccer” (and vice-versa). We compare to an oracle baseline that makes this pessimistic assumption, complementing our “No Context” ablation (which provides a comparable context-free visual reference to the clue). We give the oracle model access to the ground-truth clues, and map clues to inferences with a fine-tuned T5-Large v1.1 [52] language model, trained to perform abductive reasoning with no access to the image. Following [6], the model fits $P(\text{inference}|\text{clue})$ in a sequence-to-sequence fashion; training details are in

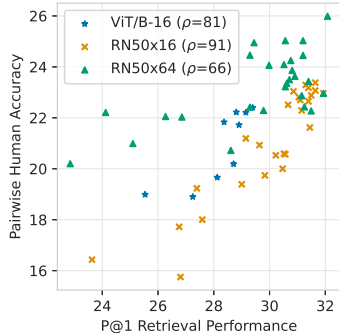


Figure 6. Validation retrieval performance ($P@1$) versus comparison accuracy for CLIP checkpoints. Retrieval performance is highly correlated with better reconstruction of human judgments.

§B. The resulting text-only clue \rightarrow inference model, when given the clue “chipped paint and rusted umbrella poles”, estimates likely inferences, for example: “the area is in a disrepair”, “this area of the town is not well maintained.”, “the city does not care about its infrastructure.”, etc. The text-only oracle under-performs vs. CLIP, as shown on Table 3, probably because global scene context cannot be fully summarized via a local referring expression. In the prior “chipped paint and rusted umbrella poles” example, the true inference, “this beach furniture does not get put inside at night”, requires additional visual context beyond the clue—chipped paint and a rusty umbrella alone may not provide enough context to infer that this furniture is beach furniture.

5.3. Error Analysis

We conduct a quantitative error analysis of our best model, multitask CLIP RN50x64 for the comparison task. For simplicity, we select 340/485 images from the validation set with a broad human agreement of above 30 according to our pairwise accuracy metric. We split images into two groups: one where the model performed above average, and one where the model performed below average, by splitting on the median accuracy. We attempt to predict into which group an image will fall. Following [51], we use a linear probe over features, and train a logistic regression model. We run a 5-fold cross-validation.

Overall, errors are difficult to predict. Surface level image/text features of the images/inferences are not very predictive of errors: relative to a 50% ROC AUC baseline, CLIP ViT-B/16 image features achieve 55%, whereas the mean SentenceBERT [53] embedding of the inference achieves 54%. While not available *a priori*, more predictive than content features of model errors are human Likert ratings: a single-feature mean human agreement model achieves 57% AUC, (more human agreement= better model performance).

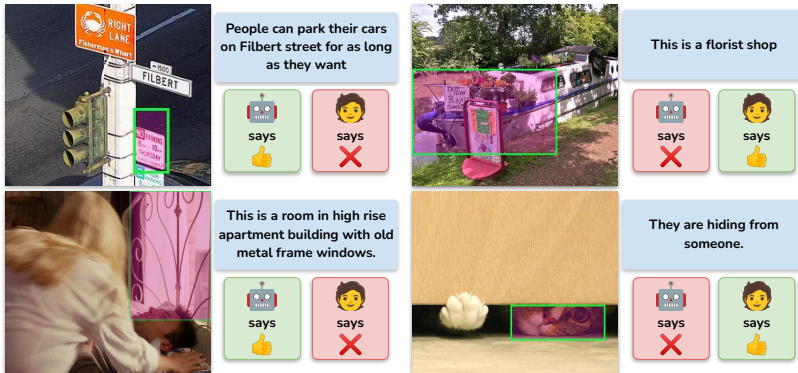


Figure 7. Error analysis: examples of false positives and false negatives predicted by our model on the comparison task’s validation set.

Figure 7 gives some examples of false positives/false negatives from the comparison task. Qualitatively speaking, the types of abductive reasoning the model falls short on are diverse. In the boat example, the model fails to notice that a florist has set up shop on a ship deck; in the window example, the model misinterprets the bars over the windows as being *outside* the building versus inside and attached to a bed-frame. The model is capable of reading some simple signs, but, as highlighted by [37], reasoning about the semantics of written text placed in images remains a challenge, e.g., a “no parking” sign is misidentified as an “okay to park” sign. Overall: the difficult-to-categorize nature of these examples suggests that the SHERLOCK corpus makes for difficult benchmark for visual abductive reasoning.

6. Conclusion

We introduce SHERLOCK, a corpus of visual abductive reasoning containing 363K clue/inference OBSERVATION PAIRS across 103K images. Our work complements existing abductive reasoning corpora, both in format (free-viewing, free-text) and in diversity (not human-centric). Our work not only provides a challenging vision+language benchmark, but also, outside of our particular tasks, we hope it can serve as a resource for studying visual abductive reasoning more broadly. Potential future work includes further exploration of:

1. Saliency: in SHERLOCK, annotators specify salient clues; how/why does saliency differ from other free-viewing setups, like image captioning?
2. Ambiguity: annotators disagree for justifiable reasons; when/why do people come to different conclusions?
3. Generative evaluations: preliminary generative modeling resulted in promising results, but generation evaluation in abductive setting, i.e., without definitive notions of correctness, remains a challenge.

Acknowledgments. This work was funded by DARPA MCS program through NIWC Pacific (N66001-19-2-4031), the DARPA SemaFor program, and the Allen Institute for AI. We additionally thank the UC Berkeley Semafor group for the helpful discussions and feedback.

References

- [1] Atocha Aliseda. The logic of abduction: an introduction. In *Springer Handbook of Model-Based Science*, pages 219–230. 2017. [2](#)
- [2] Peter Anderson, Xiaodong He, Chris Buehler, Damien Teney, Mark Johnson, Stephen Gould, and Lei Zhang. Bottom-up and top-down attention for image captioning and visual question answering. In *CVPR*, 2018. [6](#)
- [3] Stanislaw Antol, Aishwarya Agrawal, Jiasen Lu, Margaret Mitchell, Dhruv Batra, C. Lawrence Zitnick, and Devi Parikh. VQA: Visual Question Answering. In *ICCV*, 2015. [3](#)
- [4] Emily M Bender and Batya Friedman. Data statements for natural language processing: Toward mitigating system bias and enabling better science. *TACL*, 6:587–604, 2018. [15](#)
- [5] Alexander C Berg, Tamara L Berg, Hal Daume, Jesse Dodge, Amit Goyal, Xufeng Han, Alyssa Mensch, Margaret Mitchell, Aneesh Sood, Karl Stratos, et al. Understanding and predicting importance in images. In *CVPR*, 2012. [2](#), [3](#)
- [6] Chandra Bhagavatula, Ronan Le Bras, Chaitanya Malaviya, Keisuke Sakaguchi, Ari Holtzman, Hannah Rashkin, Doug Downey, Wen tau Yih, and Yejin Choi. Abductive commonsense reasoning. In *ICLR*, 2020. [2](#), [8](#)
- [7] David M Blei, Andrew Y Ng, and Michael I Jordan. Latent dirichlet allocation. *JMLR*, 3:993–1022, 2003. [4](#)
- [8] David Carson. The abduction of sherlock holmes. *International Journal of Police Science & Management*, 11(2):193–202, 2009. [1](#)
- [9] Yen-Chun Chen, Linjie Li, Licheng Yu, Ahmed El Kholy, Faisal Ahmed, Zhe Gan, Yu Cheng, and Jingjing Liu. UNITER: Universal image-text representation learning. In *ECCV*, 2020. [2](#), [6](#), [7](#)
- [10] Alexey Dosovitskiy, Lucas Beyer, Alexander Kolesnikov, Dirk Weissenborn, Xiaohua Zhai, Thomas Unterthiner, Mostafa Dehghani, Matthias Minderer, Georg Heigold, Sylvain Gelly, et al. An image is worth 16x16 words: Transformers for image recognition at scale. In *ICLR*, 2021. [7](#)
- [11] Li Du, Xiao Ding, Ting Liu, and Bing Qin. Learning event graph knowledge for abductive reasoning. In *ACL*, 2021. [2](#)
- [12] Zhiyuan Fang, Tejas Gokhale, Pratyay Banerjee, Chitta Baral, and Yezhou Yang. Video2Commonsense: Generating commonsense descriptions to enrich video captioning. In *EMNLP*, 2020. [3](#)
- [13] Noa Garcia, Mayu Otani, Chenhui Chu, and Yuta Nakashima. KnowIT vqa: Answering knowledge-based questions about videos. In *AAAI*, 2020. [3](#)
- [14] Timnit Gebru, Jamie Morgenstern, Briana Vecchione, Jennifer Wortman Vaughan, Hanna Wallach, Hal Daumé Iii, and Kate Crawford. Datasheets for datasets. *Communications of the ACM*, 2021. [4](#), [15](#)
- [15] Herbert P Grice. Logic and conversation. In *Speech acts*, pages 41–58. Brill, 1975. [2](#)
- [16] Kaiming He, Xiangyu Zhang, Shaoqing Ren, and Jian Sun. Deep residual learning for image recognition. In *CVPR*, 2016. [7](#)
- [17] Jerry R Hobbs, Mark E Stickel, Douglas E Appelt, and Paul Martin. Interpretation as abduction. *Artificial intelligence*, 63(1-2):69–142, 1993. [3](#)
- [18] Hossein Hosseini, Sreeram Kannan, Baosen Zhang, and Radha Poovendran. Deceiving google’s perspective api built for detecting toxic comments. *arXiv preprint arXiv:1702.08138*, 2017. [4](#), [14](#)
- [19] Oana Ignat, Santiago Castro, Hanwen Miao, Weiji Li, and Rada Mihalcea. WhyAct: Identifying action reasons in lifestyle vlogs. In *EMNLP*, 2021. [3](#)
- [20] Yunseok Jang, Yale Song, Youngjae Yu, Youngjin Kim, and Gunhee Kim. Tgif-QA: Toward spatio-temporal reasoning in visual question answering. In *CVPR*, 2017. [3](#)
- [21] Justin Johnson, Bharath Hariharan, Laurens Van Der Maaten, Li Fei-Fei, C Lawrence Zitnick, and Ross Girshick. Clevr: A diagnostic dataset for compositional language and elementary visual reasoning. In *CVPR*, 2017. [3](#)
- [22] Justin Johnson, Andrej Karpathy, and Li Fei-Fei. Denscap: Fully convolutional localization networks for dense captioning. In *CVPR*, 2016. [2](#)
- [23] Justin Johnson, Ranjay Krishna, Michael Stark, Li-Jia Li, David Shamma, Michael Bernstein, and Li Fei-Fei. Image retrieval using scene graphs. In *CVPR*, 2015. [3](#)
- [24] Roy Jonker and Anton Volgenant. A shortest augmenting path algorithm for dense and sparse linear assignment problems. *Computing*, 38(4):325–340, 1987. [6](#)
- [25] Sahar Kazemzadeh, Vicente Ordonez, Mark Matten, and Tamara Berg. ReferItGame: Referring to objects in photographs of natural scenes. In *EMNLP*, 2014. [5](#)
- [26] Diederik P Kingma and Jimmy Ba. Adam: A method for stochastic optimization. *arXiv preprint arXiv:1412.6980*, 2014. [14](#)
- [27] Emiel Kraahmer and Kees Van Deemter. Computational generation of referring expressions: A survey. *Computational Linguistics*, 38(1):173–218, 2012. [5](#)
- [28] Ranjay Krishna, Yuke Zhu, Oliver Groth, Justin Johnson, Kenji Hata, Joshua Kravitz, Stephanie Chen, Yannis Kalantidis, Li-Jia Li, David A. Shamma, Michael S. Bernstein, and Li Fei-Fei. Visual genome: Connecting language and vision using crowdsourced dense image annotations. *IJCV*, 2016. [3](#), [6](#), [7](#), [16](#)
- [29] Harold W Kuhn. The hungarian method for the assignment problem. *Naval research logistics quarterly*, 2(1-2):83–97, 1955. [6](#)
- [30] Jie Lei, Licheng Yu, Tamara L Berg, and Mohit Bansal. TVQA+: Spatio-temporal grounding for video question answering. In *ACL*, 2020. [3](#)
- [31] Jie Lei, Licheng Yu, Tamara L Berg, and Mohit Bansal. What is more likely to happen next? video-and-language future event prediction. In *EMNLP*, 2020. [3](#)

- [32] Tsung-Yi Lin, Michael Maire, Serge J. Belongie, James Hays, Pietro Perona, Deva Ramanan, Piotr Dollár, and C. Lawrence Zitnick. Microsoft COCO: Common objects in context. In *ECCV*, 2014. 6, 7
- [33] Jingzhou Liu, Wenhua Chen, Yu Cheng, Zhe Gan, Licheng Yu, Yiming Yang, and Jingjing Liu. Violin: A large-scale dataset for video-and-language inference. In *CVPR*, 2020. 3
- [34] Yinhan Liu, Myle Ott, Naman Goyal, Jingfei Du, Mandar Joshi, Danqi Chen, Omer Levy, Mike Lewis, Luke Zettlemoyer, and Veselin Stoyanov. RoBERTa: A robustly optimized bert pretraining approach. *arXiv preprint arXiv:1907.11692*, 2019. 5
- [35] Ilya Loshchilov and Frank Hutter. Decoupled weight decay regularization. In *ICLR*, 2019. 14
- [36] Kenneth Marino, Mohammad Rastegari, Ali Farhadi, and Roozbeh Mottaghi. OK-VQA: A visual question answering benchmark requiring external knowledge. In *CVPR*, 2019. 3
- [37] Anand Mishra, Shashank Shekhar, Ajeet Kumar Singh, and Anirban Chakraborty. OCR-VQA: Visual question answering by reading text in images. In *ICDAR*, 2019. 9
- [38] Margaret Mitchell, Simone Wu, Andrew Zaldivar, Parker Barnes, Lucy Vasserman, Ben Hutchinson, Elena Spitzer, Inioluwa Deborah Raji, and Timnit Gebru. Model cards for model reporting. In *FACCT*, 2019. 4, 14
- [39] Ilkka Niiniluoto. Defending abduction. *Philosophy of science*, 66:S436–S451, 1999. 1
- [40] Aaron van den Oord, Yazhe Li, and Oriol Vinyals. Representation learning with contrastive predictive coding. *arXiv preprint arXiv:1807.03748*, 2018. 7
- [41] Vicente Ordonez, Girish Kulkarni, and Tamara L. Berg. Im2text: Describing images using 1 million captioned photographs. In *NeurIPS*, 2011. 7
- [42] Ekaterina Ovchinnikova, Niloofar Montazeri, Theodore Alexandrov, Jerry R Hobbs, Michael C McCord, and Ritu Mulkar-Mehta. Abductive reasoning with a large knowledge base for discourse processing. In *IWCS*, 2011. 3
- [43] Dong Huk Park, Trevor Darrell, and Anna Rohrbach. Robust change captioning. In *ICCV*, 2019. 3
- [44] Jae Sung Park, Chandra Bhagavatula, Roozbeh Mottaghi, Ali Farhadi, and Yejin Choi. VisualCOMET: Reasoning about the dynamic context of a still image. In *ECCV*, 2020. 2, 3, 13
- [45] Debjit Paul and Anette Frank. Generating hypothetical events for abductive inference. In **SEM*, 2021. 2
- [46] Charles S Peirce. *Philosophical writings of Peirce*, volume 217. Courier Corporation, 1955. 2
- [47] Charles Sanders Peirce. *Pragmatism and pragmaticism*, volume 5. Belknap Press of Harvard University Press, 1965. 1, 2
- [48] Sandro Pezzelle, Claudio Greco, Greta Gandolfi, Eleonora Gualdoni, and Raffaella Bernardi. Be different to be better! a benchmark to leverage the complementarity of language and vision. In *Findings of EMNLP*, 2020. 3
- [49] Hamed Pirsiavash, Carl Vondrick, and Antonio Torralba. Inferring the why in images. Technical report, 2014. 3
- [50] Lianhui Qin, Vered Shwartz, Peter West, Chandra Bhagavatula, Jena Hwang, Ronan Le Bras, Antoine Bosselut, and Yejin Choi. Back to the future: Unsupervised backprop-based decoding for counterfactual and abductive common-sense reasoning. In *EMNLP*, 2020. 2
- [51] Alec Radford, Jong Wook Kim, Chris Hallacy, Aditya Ramesh, Gabriel Goh, Sandhini Agarwal, Girish Sastry, Amanda Askell, Pamela Mishkin, Jack Clark, et al. Learning transferable visual models from natural language supervision. *arXiv preprint arXiv:2103.00020*, 2021. 2, 7, 9, 13, 14
- [52] Colin Raffel, Noam Shazeer, Adam Roberts, Katherine Lee, Sharan Narang, Michael Matena, Yanqi Zhou, Wei Li, and Peter J Liu. Exploring the limits of transfer learning with a unified text-to-text transformer. *JMLR*, 2020. 8
- [53] Nils Reimers and Iryna Gurevych. Sentence-bert: Sentence embeddings using siamese bert-networks. In *EMNLP*, 2019. 9, 15
- [54] Shaoqing Ren, Kaiming He, Ross Girshick, and Jian Sun. Faster R-CNN: Towards real-time object detection with region proposal networks. *NeurIPS*, 2015. 6
- [55] Maarten Sap, Dallas Card, Saadia Gabriel, Yejin Choi, and Noah A Smith. The risk of racial bias in hate speech detection. In *ACL*, 2019. 4, 14
- [56] Gary Shank. The extraordinary ordinary powers of abductive reasoning. *Theory & Psychology*, 8(6):841–860, 1998. 2
- [57] Piyush Sharma, Nan Ding, Sebastian Goodman, and Radu Soricut. Conceptual captions: A cleaned, hypemymed, image alt-text dataset for automatic image captioning. In *ACL*, 2018. 7
- [58] Noam Shazeer and Mitchell Stern. Adafactor: Adaptive learning rates with sublinear memory cost. In *ICML*, 2018. 14
- [59] Kihyuk Sohn. Improved deep metric learning with multi-class n-pair loss objective. In *NeurIPS*, 2016. 7
- [60] Oyvind Tafjord, Bhavana Dalvi Mishra, and Peter Clark. ProofWriter: Generating implications, proofs, and abductive statements over natural language. In *Findings of ACL*, 2021. 2
- [61] Hao Tan and Mohit Bansal. LXMERT: Learning cross-modality encoder representations from transformers. In *EMNLP*, 2019. 2, 6, 7
- [62] Mingxing Tan and Quoc Le. Efficientnet: Rethinking model scaling for convolutional neural networks. In *ICML*, 2019. 7
- [63] Makarand Tapaswi, Yukun Zhu, Rainer Stiefelhagen, Antonio Torralba, Raquel Urtasun, and Sanja Fidler. MovieQA: Understanding stories in movies through question-answering. In *CVPR*, 2016. 3
- [64] Ashish Vaswani, Noam Shazeer, Niki Parmar, Jakob Uszkoreit, Llion Jones, Aidan N Gomez, Łukasz Kaiser, and Illia Polosukhin. Attention is all you need. In *NeurIPS*, 2017. 6
- [65] Ramakrishna Vedantam, Xiao Lin, Tanmay Batra, C Lawrence Zitnick, and Devi Parikh. Learning common sense through visual abstraction. In *ICCV*, 2015. 3
- [66] Peng Wang, Qi Wu, Chunhua Shen, Anthony Dick, and Anton Van Den Hengel. FVQA: Fact-based visual question answering. *TPAMI*, 40(10):2413–2427, 2017. 3

- [67] Peng Wang, Qi Wu, Chunhua Shen, Anton van den Hengel, and Anthony Dick. Explicit knowledge-based reasoning for visual question answering. In *IJCAI*, 2017. 3
- [68] Thomas Wolf, Lysandre Debut, Victor Sanh, Julien Chaumond, Clement Delangue, Anthony Moi, Pierric Cistac, Tim Rault, Rémi Louf, Morgan Funtowicz, Joe Davison, Sam Shleifer, Patrick von Platen, Clara Ma, Yacine Jernite, Julien Plu, Canwen Xu, Teven Le Scao, Sylvain Gugger, Mariama Drame, Quentin Lhoest, and Alexander M. Rush. Transformers: State-of-the-art natural language processing. In *EMNLP: System Demonstrations*, 2020. 14
- [69] Saining Xie, Ross Girshick, Piotr Dollár, Zhuowen Tu, and Kaiming He. Aggregated residual transformations for deep neural networks. In *CVPR*, 2017. 6
- [70] Yuan Yao, Ao Zhang, Zhengyan Zhang, Zhiyuan Liu, Tat-Seng Chua, and Maosong Sun. CPT: Colorful prompt tuning for pre-trained vision-language models. *arXiv preprint arXiv:2109.11797*, 2021. 7
- [71] Kexin Yi, Chuang Gan, Yunzhu Li, Pushmeet Kohli, Jiajun Wu, Antonio Torralba, and Joshua B Tenenbaum. CLEVRER: Collision events for video representation and reasoning. In *ICLR*, 2020. 3
- [72] Licheng Yu, Eunbyung Park, Alexander C Berg, and Tamara L Berg. Visual Madlibs: Fill in the blank image generation and question answering. In *ICCV*, 2015. 3
- [73] Licheng Yu, Patrick Poirson, Shan Yang, Alexander C Berg, and Tamara L Berg. Modeling context in referring expressions. In *ECCV*, 2016. 5
- [74] Amir Zadeh, Michael Chan, Paul Pu Liang, Edmund Tong, and Louis-Philippe Morency. Social-iq: A question answering benchmark for artificial social intelligence. In *CVPR*, 2019. 3
- [75] Rowan Zellers, Yonatan Bisk, Ali Farhadi, and Yejin Choi. From recognition to cognition: Visual commonsense reasoning. In *CVPR*, 2019. 2, 3, 6, 16
- [76] Rowan Zellers, Ximing Lu, Jack Hessel, Youngjae Yu, Jae Sung Park, Jize Cao, Ali Farhadi, and Yejin Choi. MERLOT: multimodal neural script knowledge models. In *NeurIPS*, 2021. 7, 8
- [77] Chi Zhang, Feng Gao, Baoxiong Jia, Yixin Zhu, and Song-Chun Zhu. Raven: A dataset for relational and analogical visual reasoning. In *CVPR*, 2019. 3
- [78] Hongming Zhang, Yintong Huo, Xinran Zhao, Yangqiu Song, and Dan Roth. Learning contextual causality from time-consecutive images. In *CVPR Workshops*, 2021. 3
- [79] Tianyi Zhang*, Varsha Kishore*, Felix Wu*, Kilian Q. Weinberger, and Yoav Artzi. BERTScore: evaluating text generation with bert. In *ICLR*, 2020. 5
- [80] Yuke Zhu, Oliver Groth, Michael Bernstein, and Li Fei-Fei. Visual7W: Grounded question answering in images. In *CVPR*, 2016. 3

A. SHERLOCK Data Collection and Evaluation

The dataset was collected during the month of February of 2021. The data collected is in English and HITs were open to workers originating from US, Canada, Great Britain and Australia. For data collection and qualifications, average pay for the workers was maintained at \$16-\$20 with median workers being compensated \$12/hour (our target was \$15/hour for both statistics). We hash Worker IDs to preserve anonymity. A sample of data collection HIT is shown in Figure 9 (with instructions shown in Figure 8).

A.1. Qualification of Workers

As a means for ensuring high quality annotations, 266 workers were manually selected through a qualification and training rounds. The workers were presented with three images and asked to provide three OBSERVATION PAIRS per image. Each of the worker responses were manually evaluated. A total 297 workers submitting 8 reasonable OBSERVATION PAIRS of 9 were qualified for training.

The process of creating bounding boxes and linking these boxes to the OBSERVATION PAIRS was complex enough to necessitate a training stage. For the training round, qualified workers were given a standard data collection hit (Figure 9) at a higher pay to account for the time expected for them to learn the process. An additional training round was encouraged for a small pool of workers to ensure all workers were on the page with regards to the instructions and the mechanism of the hit. 266 workers worked on and completed the training (remaining 31 did not return for the training round). In this paper, we use the term *qualified workers* to refer to the workers who have completed both the qualification and training round.

A.2. Data Collection

As described in §3, we collected a total of 363K OBSERVATION PAIRS which consist of a clue and inference. Further examples of annotations are shown in Figure 11.

Image sourcing. For VCR images, we use the subset also annotated by VisualCOMET [44]; we limit our selection to images that contain at least 3 unique entities (persons or objects). For Visual Genome, during early annotation rounds, crowdworkers shared that particular classes of images were common and less interesting (e.g., grazing zebras, sheep in pastures). In response, we performed a semantic de-duplication step by hierarchical clustering into 80K clusters of extracted CLIP ViT-B/32 features [51] and sample a single image from each resulting cluster. We annotate 103K images in total, and divide them into a training/validation/test set of 90K/6.6K/6.6K, aligned with the community standard splits for these corpora.

Bounding boxes. For each clue in an OBSERVATION PAIR, the workers were asked to draw one or more bounding boxes around image regions relevant to the clue. For example, for the clue “a lot of architectural decorations” given for the lower right image in Figure 11), the worker have chosen to box each of the architectural features separately in their own bounding box. While it was not strictly enforced, we encouraged the workers to keep to a maximum of 3 bounding boxes per clue, with allowance for more if necessitated by the image and the OBSERVATION PAIR, based on worker’s individual discretion.

Confidence scores. In addition to the free-text clue, the bounding boxes drawn in the image that localizes the clue, and the free-text inference we also collected CONFIDENCE SCORE. That is, each OBSERVATION PAIR is associated with a CONFIDENCE SCORE that rates the the likelihood of the inference holding true, given the clue. The CONFIDENCE SCORE is between 1-3, where 1 indicates the lowest confidence (e.g., an educated guess) and 3 a more confident certainty. The CONFIDENCE SCORE is not

A.3. Evaluation of Model Results

For the Comparison task, we collected human judgments across the diagnostic test set of top 10 inferences per (i, r) (§4.3). More sampling details are in § C. In the HIT, workers were presented with the images with the appropriate clue region highlighted. Then they were provided with the inferences and were asked to rate them on a likert scale of 1-3, with 1 as “irrelevant” or “verifiably incorrect”, 2 as “statement is probably true but there is a better highlighted region to support it”, and 3 as “statement is probably true and the highlighted region supports it”. A sample of evaluation HIT is shown in Figure 10.

A.4. Details on exploration of social biases

The clues and inferences we collect from crowdsource workers are abductive, and thus are uncertain. Despite this type of reasoning being an important aspect of human cognition, heuristics and assumptions may reflect false and harmful social biases. As a concrete example: early on in our collection process during a qualifying round, we asked 70 workers to annotate an image of a bedroom, where action figures were placed on the bed. Many said that the bedroom was likely to belong to a *male* child, citing the action figures as evidence. We again emphasize that our goal is to *study* heuristic reasoning, without endorsing the particular inferences themselves.

Sample analysis. While curating the corpus, we (the authors) have examined several thousand annotations. To supplement our qualitative experience, in addition, we conducted a close reading of a random sample of 250 infer-

ences. This close reading was focused on references to protected characteristics of people and potentially offensive/NSFW cases.

During both our informal inspection and close reading, we observed similar patterns. Like in other vision and language corpora depicting humans, the most common reference to a protected characteristic was perceived gender, e.g., annotators often assumed depicted people were “a man” or “a woman” (and sometimes, age is also assumed, e.g., “an old man”). Aside from perception standing-in for identity, a majority of inferences are not specifically/directly about protected characteristics and are SFW (243/250 in our sample). The small number of exceptions included: assumptions about the gender of owners of items similar to the action figure example above (1/250 cases); speculation about the race of an individual based on a sweater logo (1/250); and commenting on bathing suits with respect to gender (1/250).

Since still frames in VCR are taken from movies, some depict potentially offensive imagery, e.g., movie gore, dated tropes, etc. The images in VCR come with the following disclaimer, which we also endorse (via visualcommonsense.com): “many of the images depict nudity, violence, or miscellaneous problematic things (such as Nazis, because in many movies Nazis are the villains). We left these in though, partially for the purpose of learning (probably negative but still important) commonsense implications about the scenes. Even then, the content covered by movies is still pretty biased and problematic, which definitely manifests in our data (men are more common than women, etc).”

Statistical analysis. While the random sample analysis suggests that a vast majority of annotations in our corpus do not reference protected characteristics and are SFW, for an additional check, we passed a random set of 30K samples (10K each from training/val/test) clues/inferences through the Perspective API.¹⁴ While the API itself is imperfect and itself has biases [18, 38, 55], it nonetheless can provide some additional information on potentially harmful content in our corpus. We examined the top 50 clue/inference pairs across each split marked as most likely to be toxic. Most of these annotations were false positives, e.g., “a dirty spoon” was marked as potentially toxic likely because of the word “dirty.” But, this analysis did highlight a very small amount of lewd/NSFW/offensive content. Out of the 30K cases filtered through the perspective API, we discovered 6 cases of weight stigmatization, 2 (arguably) lewd observation, 1 dark comment about a cigarette leading to an early death for a person, 1 (arguable) case of insensitivity to mental illness, 6 cases of sexualized content, and 1 (arguable) case where someone was highlighted for wearing

¹⁴<https://www.perspectiveapi.com/>; November 2021 version.

non-traditionally-gendered clothing.

B. Additional Modeling Details

After some light hyperparameter tuning on the validation set, the best learning rate for fine-tuning our CLIP models was found to be .00001 with AdamW [26, 35]. We use a linear learning rate warmup over 500 steps for RN50×16 and ViT-B/16, and 1000 for RN50×64. Our biggest model, RN50×64, takes about 24 hours to converge when trained on 8 Nvidia RTX6000 cards. For data augmentation during training, we use pytorch’s RandomCrop, RandomHorizontalFlip, RandomGrayscale, and ColorJitter. For our widescreen CLIP variants, data augmentations are executed on each half of the image independently. We compute visual/textual embeddings via a forward pass of the respective branches of CLIP — for our widescreen model, we simply average the resultant embeddings for each side of the image. To compute similarity score, we use cosine similarity, and then scale the resulting similarities using a logit scaling factor, following [51]. Training is checkpointed every 300 gradient steps, and the checkpoint with best validation $P@1$ retrieval performance is selected.

Ablation details. For all ablations, we use the ViT-B/16 version of CLIP for training speed: this version is more than twice as fast as our smallest ResNet, and enabled us to try more ablation configurations.

A cleaner training corpus. Evaluations are reported over version 1.1 of the Sherlock validation/test sets. However, our models are trained on version 1.0, which contains 3% more data; early experiments indicate that the removed data doesn’t significantly impact model performance. This data was removed because we discovered a small number of annotators were misusing the original collection interface, and thus, we removed their annotations. We encourage follow-up work to use version 1.1, but include version 1.0 for the sake of replicability.

T5 model details. We train T5-Large to map from clues to inferences using the Huggingface transformers library [68]; we parallelize using the Huggingface accelerate package. We use Adafactor [58] with learning rate .001 and batch size 32, train for 5 epochs, and select the checkpoint with the best validation loss.

B.1. Results on Clues instead of Inferences

Whereas inferences capture abductive inferences, clues are more akin to referring expressions. While inferences are our main focus at evaluation time, SHERLOCK also contains an equal number of clues, which act as literal descrip-

	Retrieval		Localization
	im \rightarrow txt (\downarrow)	$P@1_{im \rightarrow txt}$ (\uparrow)	GT-Box/Auto-Box (\uparrow)
RN50 \times 64-inference	12.8	43.4	92.5/41.4
RN50 \times 64-clue	6.2	54.3	94.7/53.3
RN50 \times 64-multitask	5.4	57.5	95.3/54.3

Table 4. Retrieval and localization results when clues are used at evaluation time instead of inferences. This task is more akin to referring expression retrieval/localization rather than abductive commonsense reasoning. While clue retrieval/localization setups are easier overall (i.e., referring expressions are easier both models to reason about) the model trained for abductive reasoning, RN50 \times 64-inference, performs worse than the model trained on referring expressions RN50 \times 64-clue.

tions of image regions: **SHERLOCK** thus provides a new dataset of 363K localized referring expressions grounded in the image regions of VisualGenome and VCR. As a pointer towards future work, we additionally report results for the retrieval and localization setups, but instead of using a version testing on inference texts, we test on clues. We do not report over our human-judged comparison sets, because or raters only observed inferences in that case. Table 4 includes prediction results of two models in this setting: both are RN50 \times 64 models trained with widescreen processing and with clues highlighted in pixel space, but one is trained on inferences, and one is trained on clues.

C. Comparison Human Evaluation Set Details

We aim to sample a diverse and plausible set of candidate inferences for images to form our comparison set. Our process is a heuristic effort designed to elicit “interesting” annotations from human raters. Even if the process isn’t perfect for generating interesting candidates, because we solicit human ratings we show inferences to annotators and ask them to rate their plausibility, the resulting set will still be a valid representation of human judgment. We start by assuming all inferences could be sampled for a given image+region, and proceed to filter according to several heuristics.

First, we use a performant RN50 \times 16 checkpoint as a means of judging plausibility of inferences. This checkpoint achieves 18.5/20.6/31.5 im2txt/txt2im/P@1 respectively on retrieval on v1.0 of the **SHERLOCK** corpus; this is comparable to the RN50 \times 16 checkpoint we report performance on in our main results section. We use this checkpoint to score all validation/test (image+region, inference) possibilities.

Global filters. We assume that if the model is already retrieving its ground truth inference which high accuracy, the instance is probably not as interesting: for each image, we disqualify all inferences that receive a lower plausibility estimate from our RN50 \times 16 checkpoint vs. the ground truth

inference (this also discards the ground-truth inference). This step ensures that the negative inferences we sample are more plausible than the ground truth inference according to the model. Next, we reduce repetitiveness of our inference texts using two methods. First, we perform the same semantic de-duplication via hierarchical clustering as described in § 3.1: clustering is computed on SentenceBERT [53] representations of inferences (all-MiniLM-L6-v2). We compute roughly 18K clusters (corresponding to 80% of the dataset size) and sample a single inference from each cluster: this results in 20% of the corpus being removed from consideration, but maintains diversity, because each of the 18K clusters is represented. Second, we perform a hard-deduplication by only allowing three verbatim copies of each inference to be sampled.

Local filters. After these global filters, we begin the iterative sampling process for each image+region. If, after all filtering, a given image+region has fewer than 20 candidates to select from, we do not consider it further. Then, in a greedy fashion, we build-up the candidate set by selecting the remaining inference with i) the highest model plausibility ii) that is maximally dissimilar to the already sampled inferences for this image according to the SentenceBERT representations. Both of these objectives are cosine similarities in vector spaces (one between image and text, and one between text and text). We assign weights so that the image-text similarity (corresponding to RN50 \times 16 plausibility) is 5x more important than the text-text dissimilarity (corresponding to SentenceBERT diversity). After iteratively constructing a diverse and plausible set of 10 inferences for a given image under this process, we globally disqualify the sampled inferences such that no inference is sampled more than once for each image (unless it is a verbatim duplicate, in which case, it may be sampled up to 3 times).

Finally, for all of the images we are able to sample a set of 10 inferences for, we sort by how promising they are collectively according to a weighted sum of: the (globally ranked) average length of the sampled inferences, the (globally ranked) diversity of the set of 10 (measured by mean all-pairs SentenceBERT cosine sim: lower=more diverse), and 5x the (globally ranked) average plausibility according to RN50 \times 16. We collect 2 human judgments for each of the 10 inferences for the top 500 images from the val/test sets (1K total) according to this heuristic ranking. The total is 20K human judgments, which formed v1 of the **SHERLOCK** comparison corpus. v1.1 has 19K judgments.

D. Datasheet for SHERLOCK

In this section, we present a Datasheet [4, 14] for **SHERLOCK**.

1. Motivation For Datasheet Creation

- **Why was the dataset created?** **SHERLOCK** was created to support the study of visual abductive reasoning. Broadly speaking, in comparison to corpora which focus on concrete, objective facets depicted within visual scenes (e.g., the presence/absence of objects), we collected **SHERLOCK** with the goal of better understanding the types of abductive inferences that people make about images. All abductive inferences carry uncertainty. We aim to study the inferences we collect, but do not endorse their objectivity, and do not advocate for use cases that risk perpetuating them.
- **Has the dataset been used already?** The annotations we collect are novel, but the images are sourced from two widely-used, existing datasets: Visual Genome [28] and VCR [75].
- **What (other) tasks could the dataset be used for?** Aside from our retrieval/localization setups, **SHERLOCK** could be useful as a pretraining corpus for models that aim to capture information about what people might assume about an image, rather than what is literally depicted in that image. One potentially promising case: if a malicious actor were posting emotionally manipulative content online, it might be helpful to study the types of assumptions people might make about their posts, rather than the literal contents of the post itself.
- **Who funded dataset creation?** This work was funded by DARPA MCS program through NIWC Pacific (N66001-19-2-4031), the DARPA SemaFor program, and the Allen Institute for AI.

2. Data composition

- **What are the instances?** We refer to the instances as clues/inferences, which are authored by crowdworkers. As detailed in the main text of the paper, a clue is a bounding box coupled with a free-text description of the literal contents of that bounding box. An inference is an abductive conclusion that the crowdworker thinks could be true about the clue.
- **How many instances are there?** There are 363K commonsense inferences grounded in 81K Visual Genome images and 22K VCR images.
- **What data does each instance consist of?** Each instance contains 3 things: a clue, a short English literal description of a portion of the image, an inference, a short English description of an inference associated with the clue that aims to be not immediately obvious from the image content, and a bounding box specified with the region of interest.
- **Is there a label or target associated with each instance?** We discuss in the paper several tasks, which involve predicting inferences, bounding boxes, etc.

- **Is any information missing from individual instances?** Not systematically — in rare circumstances, we had to discard some instances because of malformed crowdworking inputs.
- **Are relationships between individual instances made explicit?** Yes — the annotations for a given image are all made by the same annotator and are aggregated based on that.
- **Does the dataset contain all possible instances or is it a sample?** This is a natural language sample of abductive inferences; it would probably be impossible to enumerate all of them.
- **Are there recommended data splits (e.g., training, development/validation, testing)?** Yes, they are provided.
- **Are there any errors, sources of noise, or redundancies in the dataset? If so, please provide a description.** Yes: some annotations are repeated by crowdworkers. When we collected the corpus of Likert judgments for evaluation, we performed both soft and hard deduplication steps, ensuring that the text people were evaluating wasn't overly repetitive.
- **Is the dataset self-contained, or does it link to or otherwise rely on external resources (e.g., websites, tweets, other datasets)?** It links to the images provided by Visual Genome and VCR. If images were removed from those corpora, our annotations wouldn't be grounded.

3. Collection Process

- **What mechanisms or procedures were used to collect the data?** We collected data using Amazon Mechanical Turk.
- **How was the data associated with each instance acquired? Was the data directly observable (e.g., raw text, movie ratings), reported by subjects (e.g., survey responses), or indirectly inferred/derived from other data?** Paid crowdworkers provided the annotations.
- **If the dataset is a sample from a larger set, what was the sampling strategy (e.g., deterministic, probabilistic with specific sampling probabilities)?** We downsample common image types via a semantic deduplication step. Specifically, some of our crowdworkers were rightfully pointing out that it's difficult to say interesting things about endless pictures of zebra; these types of images are common in visual genome. So, we performed hierarchical clustering on the images from that corpus, and then sampled 1 image from each of 80K clusters. The result is a downsampling of images with similar feature representations. We stopped receiving comments about zebras after this deduplication step.
- **Who was involved in the data collection process**

(e.g., students, crowdworkers, contractors) and how were they compensated (e.g., how much were crowdworkers paid)? Crowdworkers constructed the corpus via a mechanical turk HIT we designed. We our target was to pay \$15/hour. A post-hoc analysis revealed that crowdworkers were paid a median \$12/hr and a mean of \$16-20/hour, depending on the round.

- **Over what timeframe was the data collected? Does this timeframe match the creation timeframe of the data associated with the instances (e.g., recent crawl of old news articles)? If not, please describe the timeframe in which the data associated with the instances was created.** The main data was collected in February 2021.

4. Data Preprocessing

- **Was any preprocessing/cleaning/labeling of the data done (e.g., discretization or bucketing, tokenization, part-of-speech tagging, SIFT feature extraction, removal of instances, processing of missing values)?** Yes, significant preprocessing was conducted. The details are in
- **Was the “raw” data saved in addition to the preprocessed/cleaned/labeled data (e.g., to support unanticipated future uses)? If so, please provide a link or other access point to the ‘raw’ data.** The concept of “raw” data is difficult to specify in our case. We detail the data we release in the main body of the paper.
- **Is the software used to preprocess/clean/label the instances available? If so, please provide a link or other access point.** We plan to release some software related to modeling, and also have provided some appendices that detail the crowdworking labelling efforts.
- **Does this dataset collection/processing procedure achieve the motivation for creating the dataset stated in the first section of this datasheet? If not, what are the limitations?** We think so. It’s difficult to fully specify the abductive reasoning process of humans. But we think our work goes a step beyond existing corpora.

5. Dataset Distribution

- **How will the dataset be distributed?**

We make the dataset available for download via a public URL.

- **When will the dataset be released/first distributed? What license (if any) is it distributed under?**

We are working out the details of the specific license we should use and will update once we have received internal confirmation. The dataset will be released/distributed with a permissive license in the first half of 2022.

- **Are there any copyrights on the data?**

The copyright for the new annotations is held by AI2 with all rights reserved.

- **Are there any fees or access restrictions?**

No — our annotations are freely available.

6. Dataset Maintenance

- **Who is supporting/hosting/maintaining the dataset?**

The dataset is hosted and maintained by AI2.

- **Will the dataset be updated? If so, how often and by whom?**

We do not currently have plans to update the dataset regularly.

- **Is there a repository to link to any/all papers/systems that use this dataset?**

No, but if future work finds this work helpful, we hope they will consider citing this work in a way that existing web aggregators like Semantic Scholar can index.

- **If others want to extend/augment/build on this dataset, is there a mechanism for them to do so?**

People are free to remix, use, extend, build, critique, and filter the corpus: we would be excited to hear more about use cases either via our github repo, or via personal correspondence.

7. Legal and Ethical Considerations

- **Were any ethical review processes conducted (e.g., by an institutional review board)?**

After some discussion, we determined that we did not need our IRB to review this work. Crowdworking studies involving no personal disclosures of standard computer vision corpora are not required by our IRB to be reviewed by them. Specifically:

- We do not have access to the underlying personal records and will record information in such a manner that the identity of the human subject cannot readily be ascertained.
- Information generated by participants is non-identifying without turning over the personal records attached to these worker IDs.
- We do not record or include any interpersonal communication or contact between investigation and subject.

According to United States federal regulation 45 CFR 46.104, this study qualifies and as exempt and does not require IRB review.

- **Does the dataset contain data that might be considered confidential?**

Potentially, yes. Most of the content in the corpus that would be considered potentially private/confidential would likely be depicted in the images of Visual Genome (VCR are stills from movies where actors on-screen are presumably aware of their public actions). While we distribute no new images, if an image is removed from Visual Genome (or VCR), it will be removed from our corpus as well.

- **Does the dataset contain data that, if viewed directly, might be offensive, insulting, threatening, or might otherwise cause anxiety? If so, please describe why**

As detailed in the main body of the paper, we have searched for toxic content using a mix of close reading of instances and the Perspective API from Google. In doing this, we have identified a small fraction of instances that could be construed as offensive. For example, in a sample of 30K instances, we discovered 6 cases that arguably offensive (stigmatizes depicted people’s weight based on visual cues). Additionally, some of the images from VCR, gathered from popular movies, can depict potentially offensive/disturbing content. The screens can be “R Rated,” e.g., some images depict movie violence with zombies, some of the movies have Nazis as villains, and thus, some of the screenshots depict Nazi symbols. We reproduce VCR’s content warning about such imagery in § A.2.

- **Does the dataset relate to people?**

Yes: the corpus depicts people, and the annotations are frequently abductive inferences that relate to people. As detailed in the main body of the paper, 36% of inferences (or more) are grounded on people; and, many inferences that are not directly grounded on people may relate to them. Moreover, given that we aim to study abduction, which is an intrinsically subjective process, the annotations themselves are, at least in part, reflections of the annotators themselves.

- **Does the dataset identify any subpopulations (e.g., by age, gender)?**

We don’t explicitly disallow identification by gender or age, e.g., in the clues/inferences, people often will use gendered pronouns or aged language in reference to people who are depicted (e.g., “the old man”). Furthermore, while we undertook the sample/statistical toxicity analysis detailed in the main body of the paper, we have not manually verified that all 363K clue/inference pairings are free of any reference to a subpopulation. For example,

we observed one case wherein an author speculated about the country-of-origin of an individual being Morocco, clued by the observation that they were wearing a fez. Like the other observations in our corpus, it’s not necessarily the case that this is an objectively true inference, even if the fez is a hat that is worn in Morocco.

- **Is it possible to identify individuals (i.e., one or more natural persons), either directly or indirectly (i.e., in combination with other data) from the dataset?**

From the dataset we newly release, in our experience with working with the corpus, we haven’t encountered any instances where our annotators specifically identified anyone, e.g., by name. The images contained in VCR and Visual Genome that we source from do contain uncensored images of faces. But, if images are removed from those corpora, they will be removed from Sherlock as well, as we do not plan to re-host the images ourselves.

Instructions (click to expand/collapse)

Thanks for participating in this HIT!

Your task:

In this task, we are asking you to put on your detective thinking cap. Given an image, find **observable clues** that might indicate information about a person, situation, or setting that may not be necessarily obvious in the image (we will call this **indication**). You will do this in two steps.

- PART 1: Examine the image and find 3 **observable clues**.
 - ↳ An **observable clue** MUST be something in the picture (e.g., an open algebra math workbook)
 - 1. **Choose** observation number from the drop down box (1 is already chosen for you) and **write down** your clues you observed in the field to the right (What you write here will be transferred over to the PART 2).
 - 2. **Draw bounding boxes** for the clues (you may draw multiple if there are multiple things you observed).
 - 3. **Repeat** steps 1&2 for all the observations you want to make.
Then, move to Part 2 to provide indications for each of the clues you provided.
- PART 2: For each **observable clue**, provide a **indication**.
 - ↳ An **indication** is a bit of non obvious information about what the clue means to you (e.g., an open algebra math workbook might indicate there might be a high school student who was just studying)
 - **Write down** the indications.
 - **Rate** how **likely** for the **indications** to be true given **the clue**
 - **certain**: It's obvious or I'm very much certain what I said is true (I'm totally willing to bet on it!)
 - **likely**: It is likely or probable that what I said is true (both moderate and strong likelihood uncertainties belong here).
 - **possible**: It's in the realm of possibly but it's an educated guess at best.
 - We aren't looking for a particular distribution in the ratings nor do we value one rating over another. If you turn in all "possible"s for an image, for example, that's just as acceptable as turning in one of each!

Five examples are given below the instruction panel.

Bonus opportunity: you can provide up to 2 additional clues/indication sets for bonus pay.

Rules:

1. For **observable clues**:
 - Write a noun phrase: "the book", "gray skies", "a group of people"
 - When possible, please specify details relevant as to where the object, entity, or thing:
 - "the book" → "the book *under the table*"
 - "buttons" → "buttons *on the man's shirt*"
 - "a group of people" → "a group of people *in the pool*"
 - "a painting" → "a painting *hanging on the wall*"
 - "a dog" → "a dog *following a person*"
 - You can provide similar **observable clues** multiple times, but please tailor your clue to the observation made (see Example 2).
 - When **bounding the clues**, please remember: the boxes do not have to be perfect! 1-3 items in a picture is plenty for bounding. Do not spend too much time on this step!
2. For **indications**:
 - Write in complete sentences
 - Make the indications **realistic**
 - Please **DO NOT** write indications that **contradict** each other.
For example, indications like "*this is a gathering of family members*" and "*this is a work event*" cannot both be true. These are contradictions of each other. Please AVOID these.
3. At this time, we are **NOT interested in** in plain descriptions of what's going on, what people are doing, and what the people are thinking. Please see "**How to Pick Good Clues/Indications**" for further detail.
4. Please use weather related observations if it's a salient aspect of the image or you have nothing else you can talk about. Please use weather as the last resort. Example 4 observation 2 is an example of a weather observation.
5. Please avoid gendered pronouns like "he", "she", "him" or "her". If you desire, you can use "they".
6. Read through example and how-to sections below!

How to Pick Good Clues/Indications (click to expand/collapse)

Examples (click to expand/collapse)

Figure 8. Instructions for SHERLOCK data collection HIT.

PART 1: Make your observations and bound them in boxes

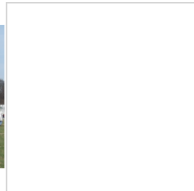
Observe image below, then:

- **STEP 1:** Choose observation number from the drop down box (1 is already chosen for you) and **write down** your observed clues in the text field to the right. (What you write here will be transferred over to the PART 2 below.)
- **STEP 2:** Draw bounding boxes in the image below. The boxes do not have to be perfect!
 - Just click and drag over parts of the you want to box.
 - 1-3 boxes are enough. You don't have to go crazy here! We just want the key bits.
 - To remove a box, hover over the top right corner of the box until you see a **X**.
- **STEP 3:** Repeat steps 1&2 for all the observations you want to make. Then, move to Part 2 to provide indications for each of the clues you provided.

Observation # **1** I spy...
(Observations 1-3 are required; 4 & 5 are bonus/optional)



Thumbnail (re)load



Zoomed selection

PART 2: Fill in the indications

Observation 1 (required):

I spy...

It might indicate that...

I think this is... possible (a stab, a guess) likely (quite to very likely) certain (willing to bet money on it)

Observation 2 (required):

I spy...

It might indicate that...

I think this is... possible (a stab, a guess) likely (quite to very likely) certain (willing to bet money on it)

Observation 3 (required):

I spy...

It might indicate that...

I think this is... possible (a stab, a guess) likely (quite to very likely) certain (willing to bet money on it)

Figure 9. Template setup for **SHERLOCK** data collection HIT. Instructions are shown in Figure 8

Instructions (click to expand/collapse)

Thanks for participating in this HIT!

Your task:

You will be presented with an image that contains a highlighted region. Then, you'll be shown **10 statements** that a machine made about the same image/region. Your job is to **rate the machine predictions**. You'll rate the predictions on a good/okay/bad scale.

- **Good:** probably or definitely correct, AND the region is the best part of the image to support the conclusion.
- **Okay:** the sentence is probably correct for the scene, BUT there is definitely a better region in the image that would support the conclusion.
- **Bad:** there is little to no evidence in the image for the conclusion, or the conclusion is verifiably false.

IMPORTANT: you MUST take the **region of the image** as a basis of deciding whether the image is **Good** or **Okay**.

NOTES:

- Please assess the statements individually.

For example, let's say you decided a statement like "The person's a high school teacher" was correct in an earlier statement. A later statement reads "The person's a professor". While in real life, both statements cannot coexist, *IF* the image is such that both statements could be probable, then it is fine to accept both statements as Good or Okay (depending on what the region contains).

- Please be forgiving of minor spelling, grammar, and plural (e.g., "man" vs. "men") errors.

Examples (click to expand/collapse)

(Click on the image to view the original.)



Machine statement 1: "\${machine_statement_1}"

- Good:** statement is true for image, the region highlighted is the best
- Okay:** statement could be true, but a different region would be better, or I can't tell for sure it's true.
- Bad:** statement is verifiably incorrect, is not justified by the image nor the region, or is irrelevant.

Machine statement 2: "\${machine_statement_2}"

- Good:** statement is true for image, the region highlighted is the best
- Okay:** statement could be true, but a different region would be better, or I can't tell for sure it's true.
- Bad:** statement is verifiably incorrect, is not justified by the image nor the region, or is irrelevant.

Figure 10. Instructions and template setup for **SHERLOCK** model evaluation HIT.

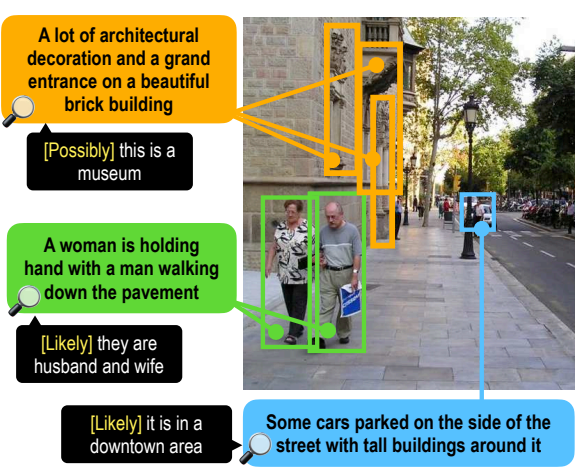
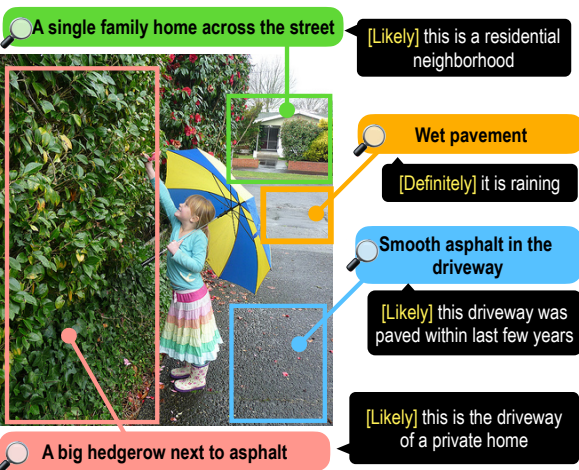
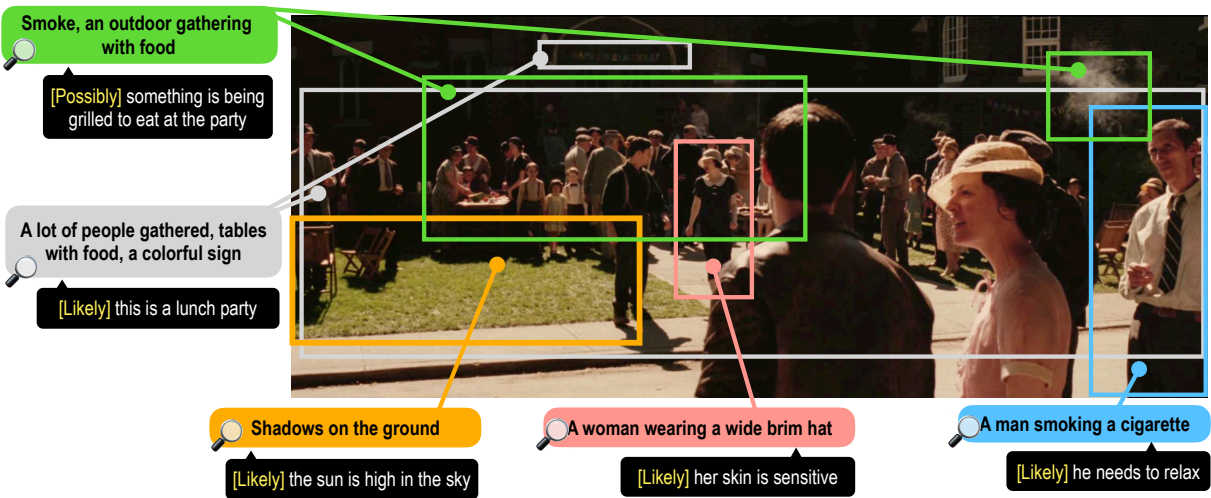
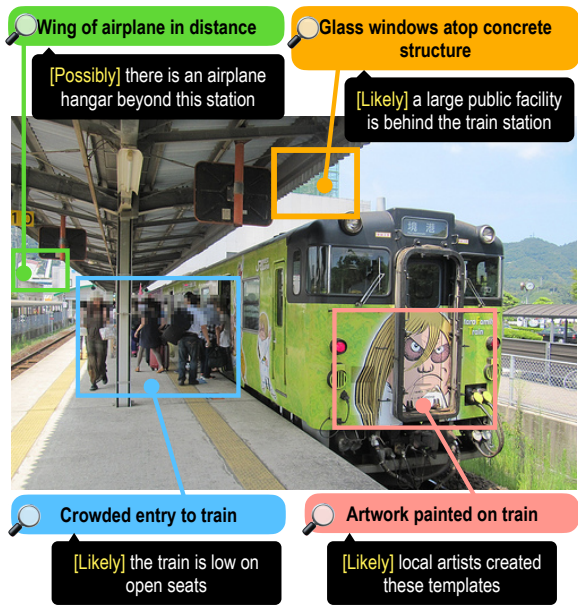
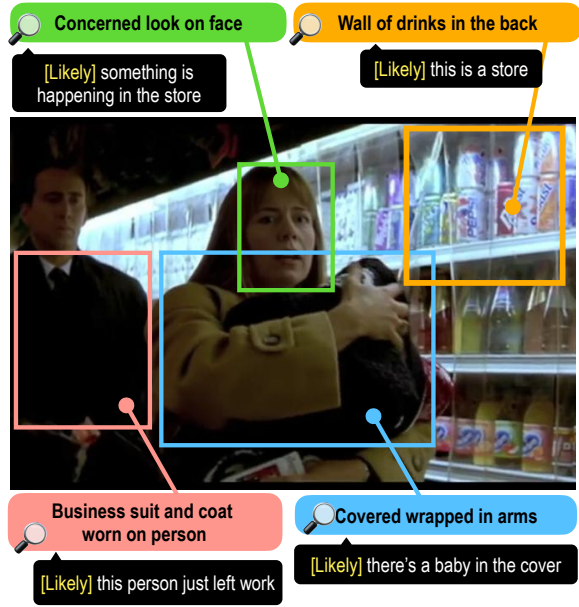


Figure 11. Examples of clues and inference pair annotations in **SHERLOCK** over images from Visual Genome and VCR. For each OBSERVATION PAIR, an inference (speech bubble) is grounded in a concrete clue (color bubble) present in an image. CONFIDENCE SCORE (in the order of decreasing confidence: “Definitely” > “Likely” > “Possibly”) for each inference is shown in yellow.